Appl. Phys. B (2017) 123:152
DOI 10.1007/s00340-017-6729-4

Applied Physics B
Lasers and Optics

Dynamical bistability of a loss modulated erbium doped fiber ring laser

Gyanendra Kumar[1,2] · **R. Vijaya**[1,3]

Received: 11 February 2017 / Accepted: 10 April 2017 / Published online: 20 April 2017

Abstract Optical hysteresis in the modulated output of an erbium doped fiber ring laser is recorded while raising and lowering the modulation index and modulation frequency, during the intra-cavity loss modulation with an intensity modulator included in the ring cavity. The analysis is done using the phase difference between the modulating signal and the laser output. The bistable output observed near the fundamental and sub-harmonic resonances can be understood by this method. The faster transition of the laser output while increasing the modulation parameters near the fundamental frequency range is contrasted with the slower dynamics at the sub- and super-harmonic frequency ranges under similar conditions by calculating the flipping time. The results based on the standard laser dynamics model provide a good match with the experiments.

1 Introduction

Erbium-doped fiber amplifiers (EDFA) and erbium-doped fiber lasers (EDFL) are well known for their utility in applications ranging from optical communication [1] to LIDAR technology [2]. While the EDFA has a prime role as the in-line amplifier in the present fiber-optic communication networks [3, 4], EDFL is emerging as a useful pump laser for environmental gas sensing [5]. Apart from these standard applications, it is noteworthy that the EDFL exhibits a large variety of dynamical behaviour, wherein optical bistability is also a possibility. Bistability in laser response has practical implications for using it in optical switches. In fiber lasers, the optical bistability was studied in the case of Nd-doped fiber laser with a modulated pump by Phillips et al. in 1987. They observed the hysteresis while raising and lowering the modulation frequency [6]. Luo et al. [7] studied the bistability in EDFL with the sinusoidal modulation of the input pump power. Shao et al. [8] reported optical bistability in EDFRL while raising and lowering the pump power. They attributed the bistability to all the photons of pump not converting to the signal wavelength due to attenuation from various components in the cavity and their different contributions while raising and lowering of the pump power. They have explained it by calculating the gain characteristic with the variation of pump power and found different threshold pump power for lasing. Recently, Martín [9] has reported bistability in a sinusoidally pump modulated EDFL with the injection of an external signal into the cavity. In spite of the extensive work on bistable response of EDFL reported using various techniques [6–10], the experimental demonstration of bistable response of EDFL under loss modulation scheme is not explored to the best of our knowledge. Loss modulation can be a better choice since it provides a better control on the nonlinear dynamics of the laser [11].

We experimentally investigated the optical bistability in erbium doped fiber ring laser (EDFRL) by modulating its cavity loss with a $LiNbO_3$ based intensity modulator in the ring driven by a sinusoidal signal. Here, our main focus is to study the dynamics of EDFRL by analysing the bistable hysteresis. We studied the bistable operation and flipping time analysis at fundamental as well as sub- and

✉ R. Vijaya
rvijaya@iitk.ac.in

[1] Department of Physics, Indian Institute of Technology Kanpur, Kanpur 208016, India

[2] Present Address: Department of Physics, Indian Institute of Technology Roorkee, Roorkee 247667, India

[3] Center for Lasers and Photonics, Indian Institute of Technology Kanpur, Kanpur 208016, India

super-harmonic frequency regions. The extent of bistability and the flipping time are found to be quite different at each of these characteristic frequencies in the laser's dynamical response. The flipping time of the laser state can be an important parameter for deciding its suitability for the switching operations.

The paper is organized as follows. The experimental details for the loss modulation are discussed in Sect. 2. In Sect. 3, a detailed experimental study of the dynamical bistability in the output response of EDFRL by tuning the modulation frequency and modulation index of the sinusoidal modulating signal. A brief description of the model used in the calculations is given in Sect. 4. The calculated results appropriate to the experiments are shown in Sect. 5. This is followed by the conclusions in Sect. 6.

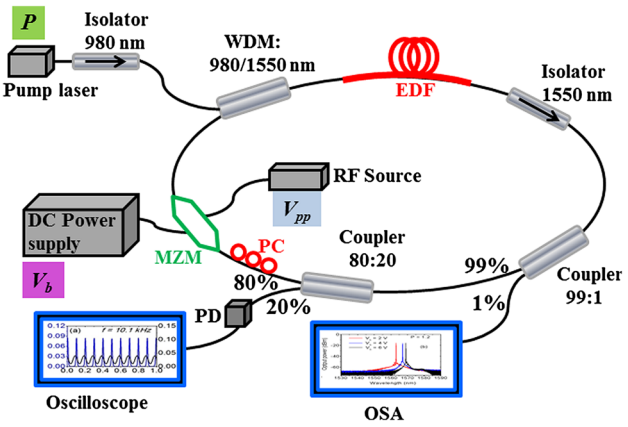

Fig. 1 Experimental set-up of the erbium doped fiber laser containing a Mach–Zehnder modulator inside the ring for cavity loss modulation

2 Experimental set-up

The schematic of the EDFRL experimental set-up is shown in Fig. 1. Here, the 8 m erbium doped fiber (EDF), having erbium concentration of 3.535×10^{25} ions/m^3 is pumped by a 980 nm wavelength laser (Lumics™) and a wavelength division multiplexer (WDM) is used to couple the 980 and 1550 nm wavelengths. An isolator in the ring operating at 1550 nm ensures a uni-directional propagating wave cavity configuration. A coupler with a splitting ratio of 99:1 helps to tap out 1% of intra-cavity power, to monitor the spectral response of the laser in an optical spectrum analyzer (OSA) (EXFO™, FTB-5240S). 99% of the intra-cavity power goes to another coupler having the splitting ratio of 80:20. The 20% part goes to an oscilloscope (Agilent™, MSO-9404A) through a high-speed photo-detector (PD) (THORLABS™, DET01CFC, sampling rate 2 GSa s^{-1}) for time domain measurements and 80% part is again fed back to the ring through the Mach–Zehnder modulator (Photline™, MXER LN). There is a polarization controller (PC) at the input of the modulator, since the connecting fibers of the modulator are polarization sensitive. Total cavity length of the laser is nearly 13 m. The bias voltage (V_b) of the modulator is fixed throughout all measurements and its value is 4.5 V provided by a DC power supply. There is an RF source which is utilized as a driving signal of the modulator. The pump power used throughout the experiment is 39.5 mW while the pump power at lasing threshold is 29.3 mW.

The ratio of pump power used in the experiments to the pump power at lasing threshold gives the pumping ratio (P) and its value is 1.35 for our experiments. With the parameters used here, the lasing wavelength of the EDFRL is 1570 nm. Throughout the manuscript, the sinusoidal modulating signal is used since it is of single frequency and it helps us to analyze the frequency–response of the driven laser in its dynamical state.

3 Experimental results and discussion

3.1 With the variation of modulation frequency

To see the time-domain response of the EDFRL, the modulator is driven at different frequencies in the range of 1–35 kHz and the laser output is recorded using the oscilloscope at each frequency step. Subsequently, the laser output is also recorded when the RF driving frequency is continuously lowered back to its low value of 1 kHz. The laser response is not identical in these two cases, constituting a bistable response at certain frequencies. The photo-detector output is shown in Fig. 2a at a fixed modulation signal amplitude of $V_{pp} = 30$ mV (modulation index (m) = 0.00018) and modulation frequency of 10 kHz for both the cases of raising and lowering frequencies. The periodicities of both the cases are the same and equal to the modulating signal. But the peak intensity in the lowering frequency case is higher. On the other hand, at a modulation frequency of 20 kHz (Fig. 2b), the period of decreasing frequency case becomes twice that of the increasing frequency case. This change of periodicity is discussed in the next paragraph. Thus, the time-domain response of the laser to its intra-cavity loss modulation can be quite dramatically different depending on the frequency value as well as depending on whether the frequency is being increased or decreased.

The complete frequency range studied here is shown in Fig. 2c depicting the differences in the raising and lowering of the modulating frequency while the RF signal amplitude is kept fixed. The peak value of the photo-detector output

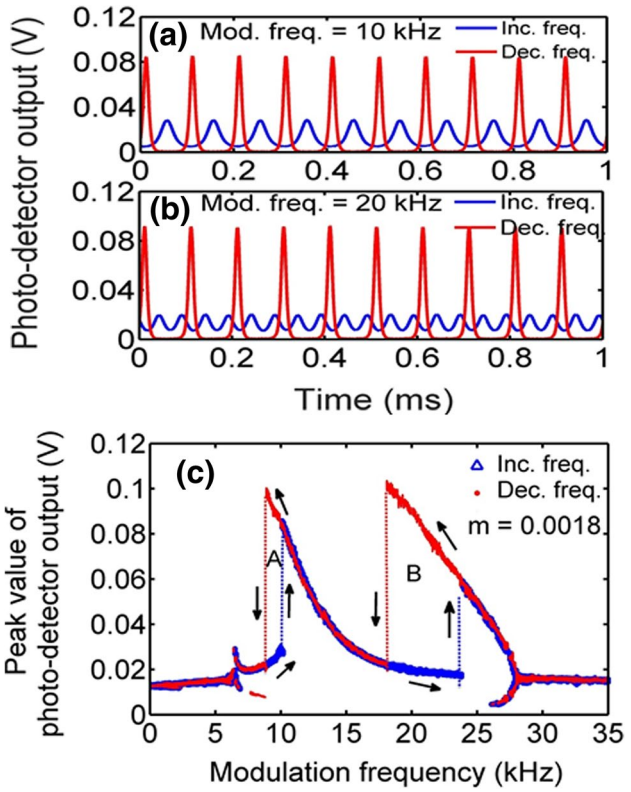

Fig. 2 Measured time series for the modulation frequency of 10 kHz (**a**) and 20 kHz (**b**), and the bistable response (**c**) of the EDFRL with the modulation frequency recorded at a fixed RF amplitude of $V_{pp} = 30$ mV ($m = 0.0018$)

corresponding to each modulation frequency is extracted from the time domain outputs through a peak search programme and is plotted at every modulation frequency in this figure. At a majority of frequency values (such as 5, 15, 20 and 30 kHz), there is only one value that signifies that all the peaks have the same peak heights. There are few frequencies (such as 6.5 and 26.5 kHz) for which there are two values that signify the presence of two peaks in the corresponding time domain output. The appearance of two peaks in the temporal output is the signature of bifurcation. This is seen for both the cases of increasing and decreasing frequency. At frequencies beyond the hysteresis range, the laser output bifurcates at the modulation frequency of 26.5 kHz and its time series exhibits alternate peaks of two different power values. On further increase in modulation frequency, the bifurcation stops at 28 kHz and its lower branch merges with the upper branch giving a periodic waveform with a single peak value. We have discussed this frequency range of bifurcation in more detail in our previous publications [12, 13].

At a fixed RF amplitude of $V_{pp} = 30$ mV ($m = 0.0018$), three resonance peaks are observed at 6.5, 10.1 and 23.9 kHz as shown in Fig. 2c (blue triangles), when the modulation frequency is increased from 1 to 35 kHz. The fundamental resonance is observed at 10.1 kHz, when the natural frequency (which is the relaxation oscillation frequency (ROF) with a value of 12.3 kHz for the chosen pumping ratio of 1.35) is comparable to the modulation frequency. Since the laser is an oscillator, its natural frequency is its relaxation oscillation frequency. At the beginning of the laser action, the absorption and emission between the relevant energy levels will alternate, leading to stabilized output through the sinusoidally varying intensity. The frequency of these sinusoidal oscillations is called the relaxation oscillation frequency. It is measured by varying the loss of the laser cavity by introducing an intensity modulator into the ring [12]. When the natural frequency is nearly twice the modulation frequency, the first super-harmonic resonance is observed at 6.5 kHz. Similarly, when the natural frequency is nearly half of the modulation frequency, a sub-harmonic resonance is observed at 23.9 kHz. When the modulation frequency is decreased from 35 kHz, the super-harmonic, fundamental and sub-harmonic resonances are observed at relatively lower frequencies of 6.4, 8.9 and 18.1 kHz, respectively, as shown in Fig. 2c (red dots). It is also noticed that the peak amplitudes reached in the lowering frequency case are higher than the values of the raising frequency case and two hysteresis regions are prominently observed, which are marked as "A" and "B" in Fig. 2.

For the hysteresis loop "A", the points to note are that (1) it is in the fundamental resonance range, (2) the hysteresis in frequency is narrow (1.2 kHz) and (3) the laser amplitudes for the increasing and decreasing frequency cases are different but by a small amount. However, for the hysteresis loop "B" in Fig. 2c, the hysteresis is in the sub-harmonic resonance range of the laser dynamics, the hysteresis in frequency is broad (5.8 kHz) and the laser amplitudes for the increasing and decreasing frequency cases are very different. This is because of the higher sensitivity of the system to the modulation frequency near the sub-harmonic frequency regime, which is discussed in an earlier work [12].

The dynamics of the laser is sensitive to the initial conditions. While raising and lowering the modulation frequency near the resonant frequencies of the laser system, the initial conditions are entirely different leading to the hysteresis in the system dynamics. On raising the modulation frequency, the laser amplitude increases drastically near the resonance frequencies and is much lower at off-resonant frequencies. When the frequency is lowered, the laser amplitude becomes very high once again but at slightly lower frequencies.

Qualitatively, one can see that with fixed modulation amplitude and a lowering of modulation frequency, the system experiences a reduced cavity loss, which increases the cavity lifetime for the field. As a result, the apparent natural

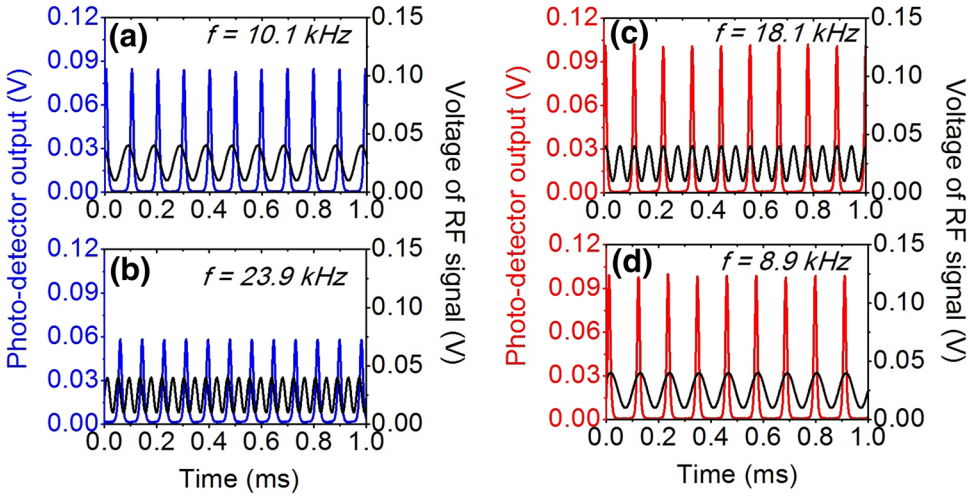

Fig. 3 Measured temporal responses (*blue* and *red lines*) of the laser and the corresponding modulating signals (*black line*) for increasing (**a**, **b**) and decreasing (**c**, **d**) modulation frequencies at a fixed modulation index of $m = 0.0018$. ($P = 1.35$)

frequency will be less than the actual. Hence, there is a shift in the fundamental resonance peak. The shift will be more for sub-harmonic frequency, since it is the integer multiple of the fundamental frequency, and much less for the super-harmonic frequency which is a fraction of the fundamental. This is clearly seen in the experimental result shown in Fig. 2c where the extent of hysteresis in the super-harmonic resonance range is much smaller. This is not analysed further here.

The pump power is an important parameter to study the dynamics of the laser. At low pump powers, the relaxation oscillation frequency of the laser remains low [14] and hence the frequency regimes for the hysteresis appear at lower frequencies. The total cavity loss is another important parameter in our study. It decides the lasing wavelength of the laser and by modulating it with an appropriate modulation index and modulation frequency, the dynamical nonlinearity in the laser can be studied. To understand the difference in the laser amplitudes at the resonance peaks while increasing and decreasing the modulation frequency, the temporal response of the RF modulating signal and the laser output are shown in Fig. 3. These time-domain data are recorded simultaneously in the experiment to see the phase difference between them.

For the loop "A" in Fig. 2c, the resonance peaks are at 10.1 and 8.9 kHz while raising and lowering the modulation frequency. The corresponding time series are shown in Fig. 3a and d, respectively. For 8.9 kHz, the time series of the laser output and modulating signal are in phase while for 10.1 kHz, the correlation is present but not so good. The laser output amplitude has reached nearly 0.09 V in both the cases as expected from Fig. 2c. For the loop "B", the modulating signal and the laser output have a phase correlation which is better for the lowering frequency case (Fig. 3c) relative to the case of increasing frequency (Fig. 3b). The study of bistability in EDFRL

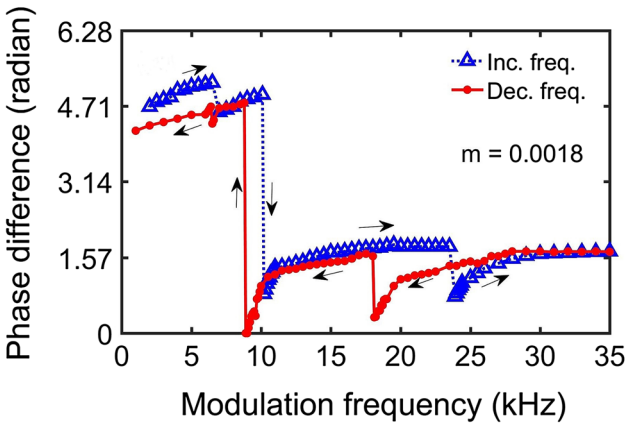

Fig. 4 Phase difference between the measured laser output and the modulating signal obtained while raising and lowering the modulation frequency

with the phase difference between the modulating signal and laser output is done under the pump modulation by Luo et al. [15] but at a much higher modulation index of 0.3. They observed that at the resonance peaks, the modulating signal and laser output were out of phase, while at the off-resonant frequencies, both were in phase.

Using Fig. 3, we have extracted this information from our data and Fig. 4 shows the phase difference between the laser output and modulating signal for raising and lowering of the modulation frequency in our work. In the case of raising frequency (blue triangles), the phase difference between the laser output and modulating signal drops sharply from $3\pi/2$ to $\pi/4$ at 10.1 kHz but recovers to $\pi/2$ at the frequency of 12 kHz, while it drops from $\pi/2$ to $\pi/4$ at 23.9 kHz but eventually recovers slowly to $\pi/2$ far from resonance. The result at 10.1 kHz is close to the expected value of phase difference of π at a fundamental resonance. However, when the modulation frequency

is lowered (red circles), the phase difference at the resonance frequencies drops nearly to zero at the shifted resonance peak positions and increases to $\pi/2$ and $3\pi/2$, respectively, at 18.1 and 8.9 kHz.

In Fig. 4, one may note that the sudden phase change for raising and lowering frequency are exactly at the resonance peaks of the laser given in Fig. 2c. While raising the modulation frequency, there is a phase change of $\pi/4$ at the sub-harmonic resonance while there is a phase change of $\pi + \pi/4$ near the fundamental. On lowering the modulation frequency, a phase change of $\pi/2$ is seen at the sub-harmonic range and $\pi + \pi/2$ at the fundamental. A phase change of π is expected near the fundamental frequency during the increase and decrease of frequency but it appears as if it over-shoots π and slowly recovers to π value eventually. One can also observe phase locked regions (marked by "M" and "N" in Fig. 4) outside the range of resonances, where the phase difference is $\pi/2$ and nearly independent of the modulation frequency. In Luo et al. [15], the phase difference is given only at some discrete modulation frequencies and hence a comparison is not possible with our results. From our work, one may state that the loss modulation technique introduces a phase difference of $\pi/4$ for the case of increasing frequency while the phase change is $\pi/2$ for the case of decreasing frequency, at the sub-harmonic resonance. Outside the resonances, the phase difference between the modulating signal and the laser output remains constant at $\pi/2$ or $3\pi/2$. If we keep increasing the modulation index, the laser output switches to the chaotic state through some higher periodic states (period-2, period-4, period-8, etc.), which we already reported in [12]. The pumping ratio in our work on loss-modulation is 1.35 which is much lower than 5.9 in the case of pump modulation [15].

In our experimental set-up, the cavity length is an important parameter. It decides the lasing wavelength and the cavity round trip time. For the cavity length chosen in our work, the cavity round trip time is 65 ns. The ROF of the laser depends on the cavity round trip time [14] and in our case, the hysteresis is observed near the ROF and its higher harmonics. Hence the frequency range of the bistable regions will shift if the cavity length is changed, since it will result in a modification of the ROF and the cavity round trip time.

3.2 With the variation of modulation index

Apart from the bistability seen during a variation of modulation frequency, EDFRL also exhibits the bistable response due to a variation of modulation index, which is shown in Fig. 5. At a fixed modulation frequency of 10 kHz, the modulation index is increased during the experiment from $m = 0.0006$ ($V_{pp} = 10$ mV) to 0.006 ($V_{pp} = 100$ mV) with a step size of 0.00012. At the modulation index of $m = 0.0025$,

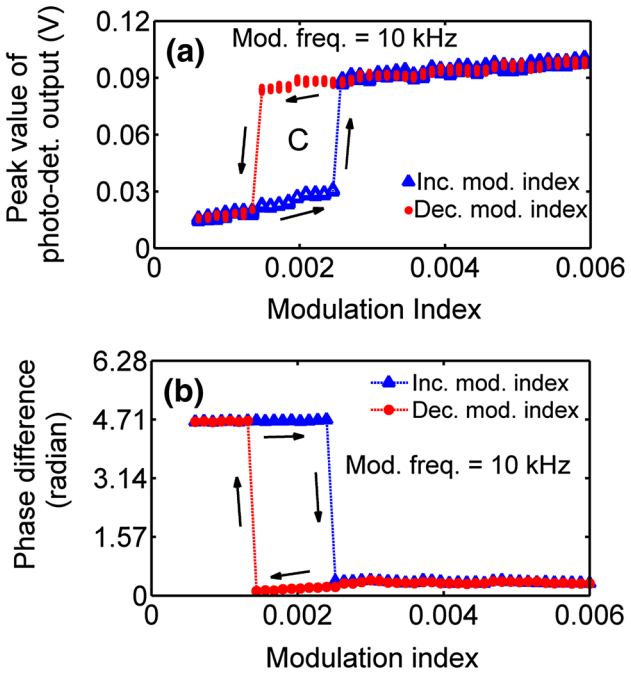

Fig. 5 **a** Measured EDFRL response at a fixed modulation frequency (10 kHz) shown with the variation of modulation index. **b** Phase difference between the laser output and the corresponding modulating signal as a function of modulation index. ($P = 1.35$)

an abrupt enhancement in the laser amplitude is observed. Furthermore, till a value of $m = 0.006$, the lasing amplitude is practically constant which is shown in Fig. 5a.

On the other hand, while decreasing the modulation index, the laser amplitude remains constant until $m = 0.0013$, when a sudden decrease in the lasing amplitude is observed. Thus, while increasing and decreasing the modulation index, the laser response is different, which results in a hysteresis loop, shown in Fig. 5a (which is marked as "C"). The modulation frequency of 10 kHz has been chosen so that the laser can exhibit the maximum laser intensity variation, for the selected span of modulation index (0.0006–0.006). A similar effect of hysteresis is expected at the harmonics of this natural frequency.

The phase difference between the laser output and the modulating signal is shown in Fig. 5b as a function of modulation index. With an increase in the modulation index, a constant phase difference of $3\pi/2$ is observed till $m = 0.0024$ ($V_{pp} = 40$ mV) and an abrupt drop to a very low value (nearly zero) is observed at $m = 0.0025$ ($V_{pp} = 42$ mV). With further increase in the modulation index, the phase difference remains unchanged up to the largest modulation index of $m = 0.006$ ($V_{pp} = 100$ mV) used in this work. It is shown with the blue triangle symbols in Fig. 5b. In the case of decreasing frequency, the phase difference is nearly the same as the increasing frequency case down to the modulation index of $m = 0.0024$

(V_{pp} = 42 mV) and then it gets lowered to zero at $m = 0.0014$ (V_{pp} = 24 mV) followed by a sudden phase change of $3\pi/2$ observed at $m = 0.0013$ (V_{pp} = 22 mV), shown with the red circles in Fig. 5b. Here, we can see that in the case of increasing the modulation index, the phase correlation between the laser output and modulating signal is better for the modulation index of 0.0025 as compared to $m = 0.0024$. It is the sole reason of enhancement in the laser amplitude. Similarly, in the case of decreasing modulation index, the phase mismatch between the laser output and modulating signal is more for the modulation index of $m = 0.0013$ relative to $m = 0.0014$. It causes the sudden decrease in the laser amplitude.

4 Calculated results and discussion

4.1 Theoretical model

Erbium doped fiber laser is a class-B laser [16] and has only two variables in time, namely the population inversion and laser amplitude. To understand its nonlinear dynamics, a third variable is inserted externally with a time-dependent cavity loss of sinusoidal modulation. The scaled rate equations used for the calculation are given below, while the details are discussed in Ref. [17–19].

$$\frac{dx}{d\theta} = s + gx(y - \alpha) \tag{1}$$

$$\frac{dy}{d\theta} = a - y(x + 1 + d) \tag{2}$$

Here, x, y, θ, s and α are the scaled parameters and represent laser amplitude, population inversion, time, spontaneous emission rate and cavity loss, respectively, while a and d are dependent on the pumping rate, and g is a constant. To incorporate the loss modulation, the parameter α, which is indicative of loss, is varied sinusoidal in time. The functional form of the modulating sinusoidal signal is $\alpha = \alpha_0(1 + m \sin(2\pi\nu\theta))$. Here, α_0 is indicative of the total passive cavity loss when there is no external modulation and m is the modulation index referred in the earlier section. For all the calculations, the parameters used are appropriate to the experiments. Even though there are other models which include excited state absorption and a few other factors, we have used the simplest model available to analyze the data due to our use of very low pumping ratio (~ 1.35) and the choice of 980 nm for the pump wavelength. The values of various scaled parameters and constants used in the calculations are $\alpha_0 = 11$, $s = 0.3$, $g = 1.2 \times 10^5$, $a = 19.4$ and $d = 0.24$. These parameters are appropriate to the experiment and account for the insertion losses of various components of the cavity, the approximate values of absorption/emission cross-sections and the extent of population inversion.

4.2 With the variation of modulation frequency

The time–domain response of EDFRL is calculated using the Eqs. 1 and 2, and different initial conditions are taken to model the cases of raising and lowering frequency. The values of the parameters x and y at any given frequency are taken as the initial conditions for the next consecutive frequency. The initial conditions while starting the calculation are $x = 0.001$ and $y = 0.001$. The step size of 0.1 kHz is used throughout the paper for the modulation frequency. At a fixed modulation index of $m = 0.00022$, the calculated output response of the laser while raising and lowering the modulation frequency is shown in Fig. 6a. On increasing the modulation frequency, the system exhibits resonances at 6.5, 10.9 and 24.8 kHz. While decreasing the modulation frequency, the resonance peaks are at 5.6, 8.5 and 17.3 kHz. Similar to the experiment, two hysteresis loops with frequency spreads of 2.4 and 7.5 kHz are observed and marked as "A1" and "B1" in Fig. 6a. The bistable response is also observed for the super-harmonic frequency range but for a very small frequency span of 0.9 kHz.

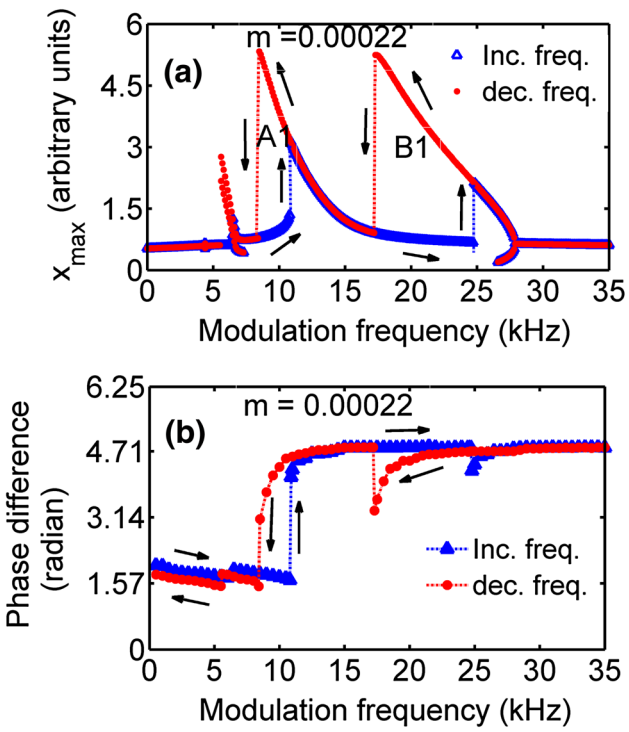

Fig. 6 **a** Calculated response of the EDFRL at different modulation frequencies. **b** Phase difference between the calculated laser output and modulating signal while raising and lowering the modulation frequency ($m = 0.00022$, $P = 1.35$)

The trends of resonance peaks are quite similar to the experiment, except for a slight change in the frequency values at the resonance peaks. There is also a discrepancy in the precise values of the modulation indices used in the experiment and in the calculations. This is because a few parameters such as the values of absorption/emission cross-section and population inversion used in the calculations are estimates from the experiment and are not very precise. Moreover, there are several hidden losses due to the presence of various components in the experiment that are not accounted in the calculation. The model is also very basic and has a scalar approach meant for a single longitudinal mode laser. Due to these inherent features, a precise matching on a quantitative level is beyond the model. But the values of modulation indices used here are validated through the relaxation oscillation frequency calculated from them and very precisely matched with the experiment [12].

The phase difference between the laser output and the corresponding modulating signal is shown as a function of modulation frequency in Fig. 6b. In the case of increasing modulation frequency, a sudden increase of the phase difference of nearly π between the laser output and modulating signal is observed at 10.9 kHz. At the frequency of 24.5 kHz, a lowering in the phase difference by $\pi/4$ is observed. For the case of decreasing modulation frequency, a phase change of $\pi/2$ and π are observed at the modulation frequencies of 17.2 and 8.5 kHz.

The phase difference between the laser output and the modulating signal appear to be somewhat different as compared to the experimental results shown in Fig. 4. But there are similarities. Far from the resonances, the phase difference is $\pi/2$ or $3\pi/2$ as in the case of the experiment. The phase change of π near the fundamental is very clear in the computed result but it seems to overshoot π in the experiment before slowly recovering to π value. One distinct difference is the decrease in phase difference at the resonance frequencies in the experiment, while the phase difference is increased in the computational result. This is because with the modulation of loss, the intra-cavity loss value is reduced at the rising edge of sinusoidal signal for the chosen bias voltage of the modulator. But in the calculation, the rising edge of the sinusoidal wave increases the loss. This aspect is not of much consequence. Apart from this, the model ignores the role of noise in the response of the system. But in the experimental situation, the presence of amplified spontaneous emission (ASE) is definitely playing a role [20].

4.3 With a variation of modulation index

Theoretically calculated bistable response of EDFRL due to a variation in modulation index is shown in Fig. 7a.

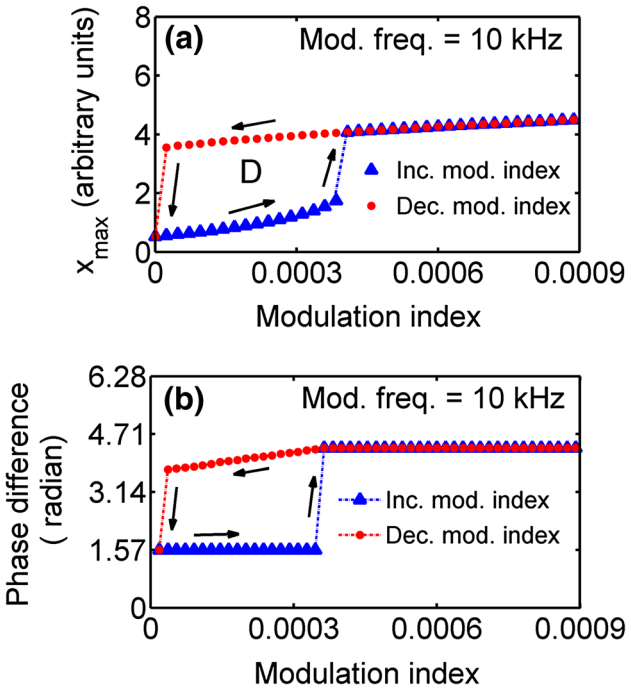

Fig. 7 **a** Response of the EDFRL calculated at a fixed modulation frequency of $f = 10$ kHz and a variation of modulation index. **b** Phase difference between the laser output and corresponding modulating signal as a function of modulation index. ($P = 1.35$)

At a fixed modulation frequency of $f = 10$ kHz, and the modulation index varying from 0 to 0.0004, the laser amplitude increases slowly followed by an abrupt jump at $m = 0.00041$. While decreasing the modulation index from 0.0009 to 0, the laser amplitude decreases slowly retracing the trends seen during the increase, and then it decreases suddenly at $m = 0.00002$. As a result, a hysteresis loop is observed, which is marked as "D" in Fig. 7a. The phase difference between the laser output and the modulating signal is shown in Fig. 7b. On increasing the modulation index, the phase difference remains constant at $\pi/2$ up to the value of $m = 0.00038$, then shows an abrupt increase to $3\pi/2$ at the value of $m = 0.00040$ and remains constant henceforth up to the maximum modulation index of $m = 0.0009$. It is shown with blue triangles in Fig. 7b. While decreasing the modulation index, the phase difference remains the same ($3\pi/2$) as the increasing case down to $m = 0.00040$, and then it slowly decreases to $5\pi/4$ at the modulation index of $m = 0.00003$ followed by a sudden decrease to $\pi/2$ (or a change of $3\pi/4$) at $m = 0.00002$ shown with red circles in Fig. 7b.

There is a good agreement between the experimental and calculated results in terms of trends except for the discrepancy in the modulation index values referred earlier. In addition, the phase difference between the calculated laser

response and the modulating signal is not exactly π perhaps because the chosen frequency (10 kHz) is not the precise value of the fundamental resonance frequency.

In any bistable system, the slow response of switching of its state near the transition points has significant practical implications. This slow response is known as "critical slowing down" [21]. The critical slowing down in the case of loss modulated CO_2 laser was reported at the boundaries of two different dynamical regions by Papoff et al. [22]. To check how quickly our laser switches its state with the change of modulation frequency, the flipping time is calculated at different modulation frequencies. Here, the flipping time is defined as the time span in which the laser switches from one output state to another output state. The initial conditions are very crucial. Hence we took initial conditions as relevant while increasing and decreasing the modulation frequency.

In the calculation of flipping time, the reference frequency is the initial frequency of the transition point. In the raising frequency case, the reference frequency is the frequency of lower laser output state while in the lowering frequency case, the reference frequency is the frequency of higher laser output state. The reference frequency selection is consistent throughout all flipping time calculations. The initial conditions are taken at a frequency which is 0.1 kHz before the reference frequency (0.1 kHz is the step size in the calculation of bistable response). So in the case of raising frequency, the frequency at which the initial conditions are taken is lower by 0.1 kHz and it is higher by 0.1 kHz in the case of lowering frequency. Here the inverse of flipping

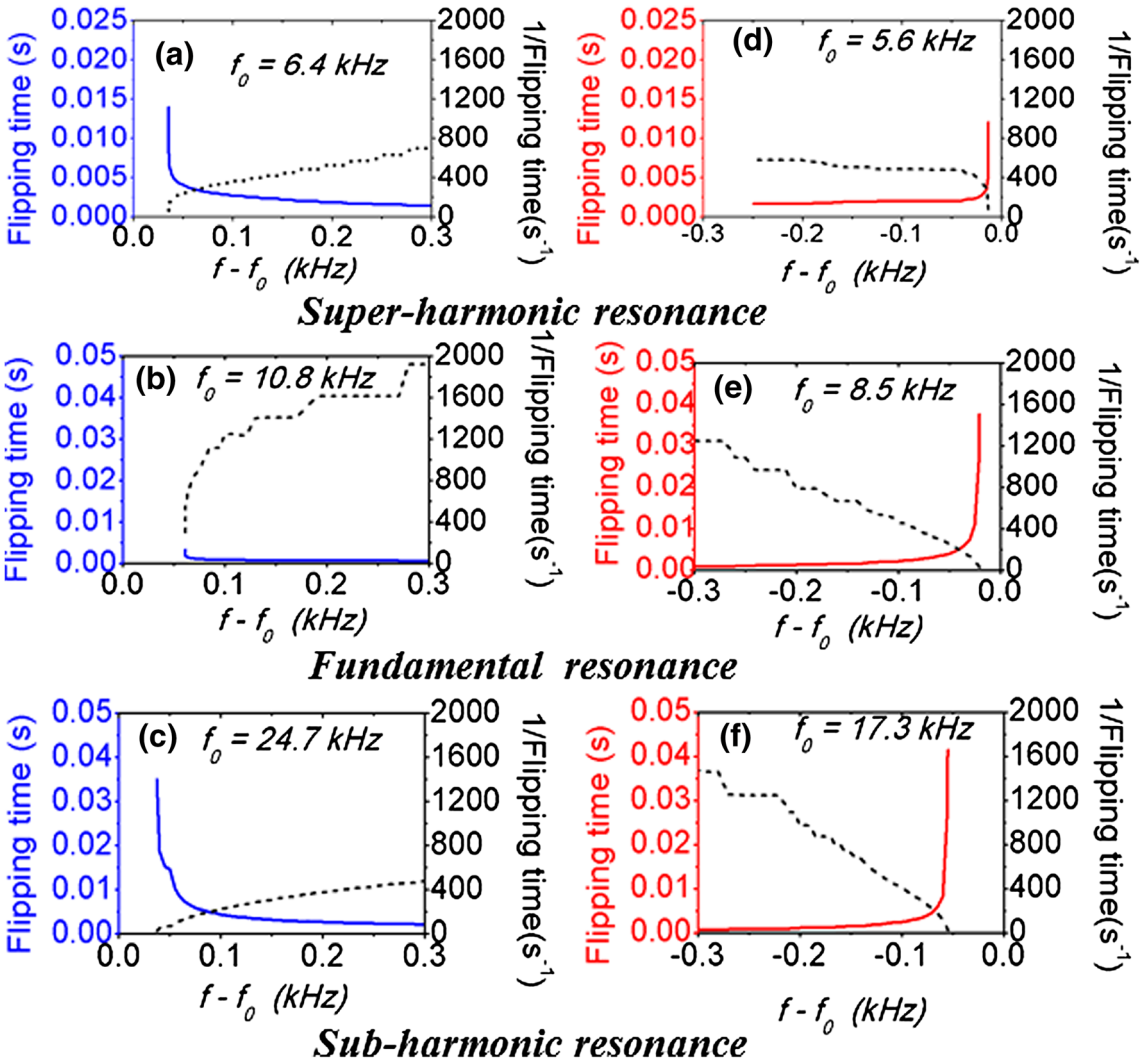

Fig. 8 Flipping time calculated as a function of frequency while increasing (**a**–**c**) and decreasing (**d**–**f**) of modulation frequency in the fundamental resonance regime at a modulation index of $m = 0.00022$. f_0 is the reference frequency. The inverse of flipping time is shown with a dashed line in every figure

time is also plotted in the right y-axis to see the time variation clearly in the case of very steep curves at transition points.

The flipping times corresponding to the super-harmonic resonance frequencies of 6.5 and 5.6 kHz while increasing and decreasing the modulation frequency are shown in Fig. 8a and d, respectively. The initial conditions are taken at 6.3 and 5.7 kHz in the cases of increasing and decreasing frequency, respectively. The flipping time curve is steeper for the case of decreasing frequency (red line), which indicates that the change of state is faster while decreasing the modulation frequency.

The flipping times for the fundamental resonance regime are shown in Fig. 8b and e. The initial conditions are taken at 10.7 and 8.6 kHz while increasing and decreasing frequencies, respectively. Here in the case of increasing frequency, we have steeper curves. The transition from one state to the other state is quicker in the case of increasing frequency (Fig. 8b) at fundamental resonance, which occurs even for very small modulating signal amplitude.

The flipping times for the sub-harmonic resonance regime are shown in Fig. 8c and f. The initial conditions are taken at 17.4 and 24.6 kHz in the case of increasing and decreasing frequencies, respectively. The flipping time variation with the frequency is steeper in the case of decreasing frequency.

The states having small flipping time can be used for fast switching applications and larger flipping time is analogous to the critical slowing down. The critical slowing down is a process in which the system response becomes extremely slow near the transition points of the bistable regime [21] and this characteristic can be utilized to develop optical buffers. It has a few more practical applications in optical delay lines, pulse filtering applications, and pulse lengthening/compressing configurations [23]. The periodically modulated lasers exhibit bistable response for the frequency of external modulation close to the natural frequency as well as its higher harmonics [24]. To achieve the bistable state in the sub-harmonic resonance regime which is relatively easier than the fundamental resonance regime [25] is clearly established through our work. The bistability is also known to get enhanced in the presence of external noise [26].

One more aspect of bistability can be tested using our calculations. We calculated the frequency range of hysteresis at different pumping ratios and modulation indices. At a fixed (and very low) pumping ratio, such as $P = 1.20$, the frequency ranges of the bistable regime for the fundamental and sub-harmonic frequencies remain nearly constant but shift towards the lower frequency side if the modulation index is increased. However, at slightly higher pumping ratios, such as $P = 1.65$, the frequency range of bistability widens significantly at higher modulation indices. This is a consequence of the increased nonlinearity in the dynamical behaviour which is easily achieved at higher pumping ratios [11], leading us to conclude that the pumping ratio is a parameter of higher significance in controlling the bistable range.

5 Conclusion

A bistable response is observed in the EDFRL while raising and lowering the amplitude or frequency of the RF signal modulating its intra-cavity loss. As a result, hysteresis is observed near the fundamental as well as sub- and super-harmonic frequency ranges of the laser oscillator response function. The hysteresis effect is the largest in the subharmonic frequency range. The underlying physics and the consequent effects are analysed by calculating the phase difference between the laser output and modulating signal while raising and lowering the modulation frequency and modulation index, as well as by calculating the flipping time for the change of state. All the measured results are supported with the calculated results. The bistable nature of EDFRL can help in configuring it for the development of optical buffers.

References

1. E. Desurvire, *Erbium-doped fiber amplifiers: principles and applications* (Wiley Interscience, New Jersey, 2002)
2. U. Sharma, C.S. Kim, U. Jin, Kang, Highly stable tunable dual-wavelength Q-switched fiber laser for DIAL applications. IEEE Phot. Techn. Lett. **16**, 1277–1279 (2004)
3. J.G. Wu, Z.M. Wu, Y.R. Liu, L. Fan, X. Tang, G.Q. Xia, Simulation of bidirectional long-distance chaos communication performance in a novel fiber optic chaos synchronization system. J. Lightwave Technol. **31**, 461–467 (2013)
4. J.G. Wu, Z.M. Wu, X. Tang, L. Fan, W. Deng, G.Q. Xia, Experimental demonstration of LD-based bidirectional fiber-optic chaos communication. IEEE Photon. Technol. Lett. **25**, 587–590 (2013)
5. S. Yao, S.Y. Chen, A. Pal, K. Bremer, B.O. Guan, T. Sun, K.T.V. Grattan, Compact Tm-doped fiber laser pumped by a 1600 nm Er-doped fiber laser designed for environmental gas sensing. Sens. Actuators, A **226**, 11–20 (2015)
6. M.W. Phillips, H. Gong, A.I. Ferguson, D.C. Hanna, Optical chaos and hysteresis in a laser-diode pumped Nd-doped fibre laser. Opt. Commun. **61**, 216–218 (1987)
7. L.G. Luo, T.J. Tee, P.L. Chu, Chaotic behaviour in erbium-doped fiber-ring lasers. J. Opt. Soc. Am. B **15**, 972–978 (1998)
8. J. Shao, S. Li, Q. Shen, Z. Wu, Z. Cao, J. Gu, Experiment and theoretical explanation of optical bistability in a single erbium doped fiber ring laser. Opt. Exp. **15**, 3673–3679 (2007)
9. J.C. Martín, Bistability in an erbium doped fiber laser controlled by a coupled external signal. IEEE Photon. Technol. Lett. **27**, 292–294 (2016)
10. I.J. Sola, J.C. Martín, J.M. Alvarez, Nonlinear response of a unidirectional erbium-doped fiber ring laser to a sinusoidally modulated pump power. Opt. Commun. **212**, 359–369 (2002)
11. G. Kumar, R. Vijaya, Control of dynamics in loss-modulated erbium doped fiber ring laser. J. Opt. Soc. Am. B **34**, 574–582 (2017)

12. G. Kumar, R. Vijaya, Dynamical features of loss and pump modulation in an erbium-doped fiber ring laser. J. Opt. **17**, 125402–125411 (2015)
13. G. Kumar, R. Vijaya, Dynamics of erbium doped fibre ring laser under cavity-loss modulation. Phys. D **304–5**, 34–41 (2015)
14. A.E. Siegman, *Lasers* (University Science Books, Mill Valley, 1986)
15. L. Luo, T.J. Tee, P.L. Chu, Bistability of erbium-doped fiber laser. Opt. Commun. **146**, 151–157 (1998)
16. A. Uchida, *Optical Communication with Chaotic Lasers* (Wiley-VCH Verlag, Weinheim, 2012)
17. J.M. Saucedo-Solorio, A.N. Pisarchik, A.V. Kir'yanov, V. Aboites, Generalized multistability in a fiber laser with modulated losses. J. Opt. Soc. Am. B **20**, 490–496 (2003)
18. W. Koechner, *Solid-State Laser Engineering* (Springer-Verlag, New York, 1976)
19. A.V. Kir'yanov, V.N. Filipov, A.N. Starodumov, CW-pumped erbium-doped fiber laser passively *Q*- switched with a Co^{2+}: ZnSe crystal: modeling and experimental study. J. Opt. Soc. Am. B **19**, 353–359 (2002)
20. G. Stewart, G. Whitenett, S. Sridaran, V. Karthik, Investigation of the dynamic response of erbium doped fiber lasers with potential applications for sensors. IEEE J. Lightwave Technol. **25**, 1786–1796 (2007)
21. R. Bonifacio, P. Meystre, Critical slowing down in optical bistability. Opt. Commun. **29**, 131–134 (1979)
22. F. Papoff, D. Dangoisse, E. Polte-Hanoteau, P. Glorieux, Chaotic transients in a CO_2 laser with modulated parameters: critical slowing down and crisis induced intermittency. Opt. Commun. **67**, 358–362 (1988)
23. H.A. Al-Attar, H.A. MacKenzie, Critical slowing-down phenomena in an InSb optically bistable etalon. J. Opt. Soc. Am. B **3**, 1157–1163 (1986)
24. T. Erneux, S.M. Baer, Subharmonic bifurcation and bistability of periodic solutions in a periodically modulated laser. Phys. Rev. A **35**, 1165–1171 (1987)
25. T. Erneux, P. Glorieux, *Laser Dynamics* (Cambridge University Press, New York, 2010)
26. G. Vemuri, R. Roy, Stochastic resonance in a bistable ring laser. Phys. Rev. A **39**, 4668–4674 (1989)